The EMBO Journal Vol.19 No.1 pp.84–93, 2000

Rhythmic opening and closing of vesicles during constitutive exo- and endocytosis in chromaffin cells

A.W.Henkel, H.Meiri[1], H.Horstmann[2], M.Lindau[3] and W.Almers[4,5]

Max-Planck-Institute for Medical Research, Jahnstrasse 29, D-69120 Heidelberg, Germany, [1]Hebrew University-Hadassah Medical School, Jerusalem, Israel, [2]IMCB Institute of Molecular and Cell Biology, 30 Medical Drive, 117609 Singapore, [3]Applied and Engineering Physics, Cornell University, 217 Clark Hall, Ithaca, NY and [4]Vollum Institute, 3181 SW Sam Jackson Park Road, Portland, OR 97201, USA

[5]Corresponding author
e-mail: almersw@ohsu.edu

Constitutive exo- and endocytic events are expected to increase and diminish the cell surface area in small spontaneous steps. Indeed, cell-attached patch–clamp measurements in resting chromaffin cells revealed spontaneous upward and downward steps in the electrical capacitance of the plasma membrane. The most frequent step size indicated cell surface changes of <0.04 μm², corresponding to vesicles of <110 nm diameter. Often downward steps followed upward steps within seconds, and vice versa, as if vesicles transiently opened and closed their lumen to the external space. Transient openings and closings sometimes alternated rhythmically for tens of seconds. The kinase inhibitor staurosporine dramatically increased the occurrence of such rhythmic episodes by making vesicle closure incomplete and by inhibiting fission. Staurosporine also promoted transient closures of large endocytic vesicles possibly representing remnants of secretory granules. We suggest that staurosporine blocks a late step in the endocytosis of both small and large vesicles, and that endocytosis involves a reaction cascade that can act as a chemical oscillator.

Keywords: chemical oscillator/membrane capacitance/rapid freezing/staurosporine

Introduction

Through exo- and endocytosis, cells release and take up soluble material as well as adding and retrieving plasma membrane. The mechanisms of exo- and endocytosis are not completely understood. Much information on exocytosis has been gained by studying single exocytic events in real time by electrophysiological techniques. Regulated exocytosis of large dense-core vesicles (LDCVs) increases the cell surface area in steps, as has been documented by measuring the electrical capacitance of the plasma membrane. Such studies were carried out in a variety of cells, among them mast cells (Fernandez *et al.*, 1984; Breckenridge and Almers, 1987; Alvarez de Toledo *et al.*, 1993), eosinophils (Scepek and Lindau, 1993), neutrophils (Lollicke *et al.*, 1995), melanotrophs (Zupancik *et al.*, 1995) and chromaffin cells (Albillos *et al.*, 1997; Ales *et al.*, 1999). In all these studies, exocytic fusion appeared reversible, in that step increases in cell surface area sometimes were followed by step decreases of essentially equal amplitude. The membrane retrieval following triggered exocytosis can also result in measurable step decreases in cell surface area (Neher and Marty, 1982; Rosenboom and Lindau, 1994; Thomas *et al.*, 1994).

Apart from regulated exocytosis and the ensuing endocytosis, endocrine and other cells carry out constitutive exocytosis (Kelly, 1985) and endocytosis (Seaman *et al.*, 1996). Constitutive endocytosis is thought to occur by vesicles much smaller than LCDVs, as does constitutive exocytosis (Bursztajn and Fischbach, 1984; Griffiths *et al.*, 1985). Cell-attached capacitance measurements have sufficient sensitivity to detect the small steps expected to result from single events in constitutive endo- and exocytosis (Lollicke *et al.*, 1995; Kreft and Zorec, 1997). Here we use this method to investigate constitutive exo- and endocytosis in chromaffin cells. We detected a slow constitutive membrane turnover caused by vesicles with a diameter of <110 nm. Both exo- and endocytic events seem reversible, in that a significant portion of exo- and endocytic events appear transient. Surprisingly, exo–endocytic organelles can lapse into a state where they rhythmically make and break connections with the cell surface. Previous results have suggested that staurosporine causes exocytic events to become transient (Henkel and Betz, 1995). Here we show that the drug encourages vesicles to close and re-open rhythmically, consistent with the idea that the drug inhibits a late step in vesicle fission.

Results

Cell-attached recording reveals stepwise changes in cell surface area

Chromaffin cells in standard bath solutions are at rest. Their plasma membrane potential is so negative that calcium channels are shut, and exocytosis of dense-core granules is not expected. Nonetheless, we observed spontaneous events presumably representing single constitutive exo- and endocytic events. Figure 1 illustrates the first 5 min of a typical experiment. Figure 1A plots the capacitance of the patch (ΔC) against time, as well as the conductance (ΔG) and the patch current (I). ΔC and ΔG represent out-of-phase and in-phase components, respectively, of the sinusoidal patch current driven by a sinusoidal voltage. With the phase properly set (see Materials and methods), ΔC assays changes in the area of plasmalemma in the patch. The ΔG trace tracks patch conductance changes due to the opening of ion channels, as well as changes in the electrical resistance of aqueous openings (fusion and fission pores) connecting exo- and endocytic vesicles with the external space. At this reso-

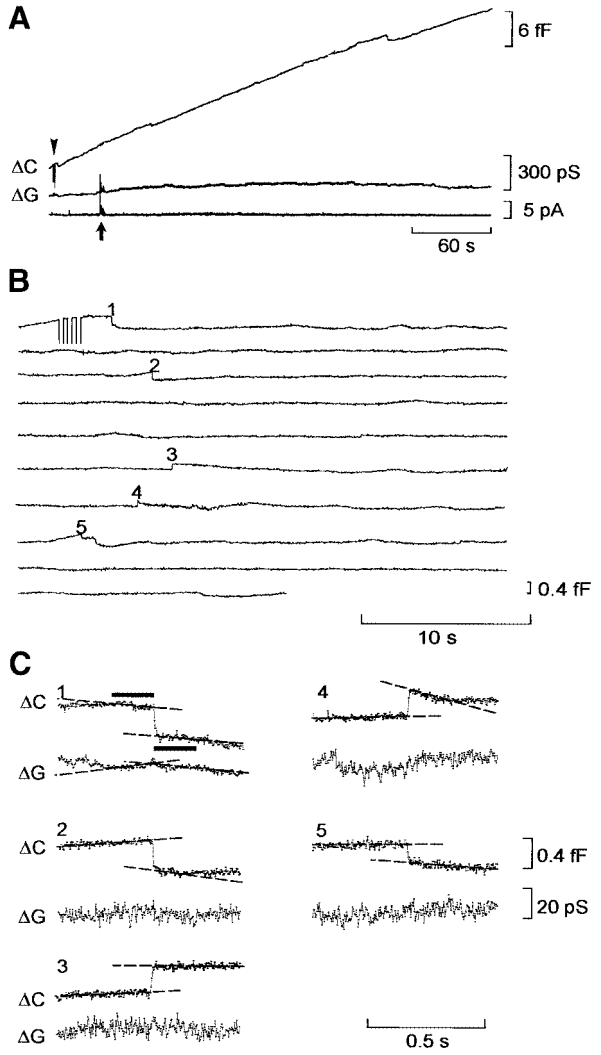

Fig. 1. Capacitance steps in chromaffin cells. (**A**) Capacitance (ΔC), conductance (ΔG) and current (I) traces in a cell-attached recording. Arrowhead, 3 fF capacitance calibration marks. Arrow, a temporary seal instability or ion channel opening caused an inward current and a simultaneous conductance increase. In the original recording, they were accompanied by slight ΔC deflections; these were removed by phase-shifting the ΔC and ΔG traces by –7° relative to ϕ_0 (see Materials and methods). (**B**) The ΔC trace in (A) after subtraction of a sloping baseline and at higher magnification. Steps labeled 1–5 passed our step selection criteria, other deflections did not. (**C**) Steps 1–5 in (B) magnified. C1 shows details of the analysis (see Materials and methods). Regression lines were fitted to the sections of both ΔC and ΔG traces that are marked by horizontal bars. Their vertical distance at the step position defines the amplitude of the ΔC and ΔG steps, if any. Standard bath solution.

lution, the most prominent features of the ΔC trace are the downward calibration marks at the beginning of the trace (arrowhead) and a slow upward drift. It was gradual, not observed in all recordings and could be increased by making the potential in the pipet negative and thereby depolarizing the membrane patch. Atomic force microscopy has shown that excised membrane patches and vesicles bulge more deeply into the pipet when a negative potential is applied to the pipet (Hörber *et al.*, 1995). Hence the upward drift in Figure 1A probably represents plasmalemma slowly moving into the pipet as an expanding bulge.

The ΔG trace remained flat except for a temporary

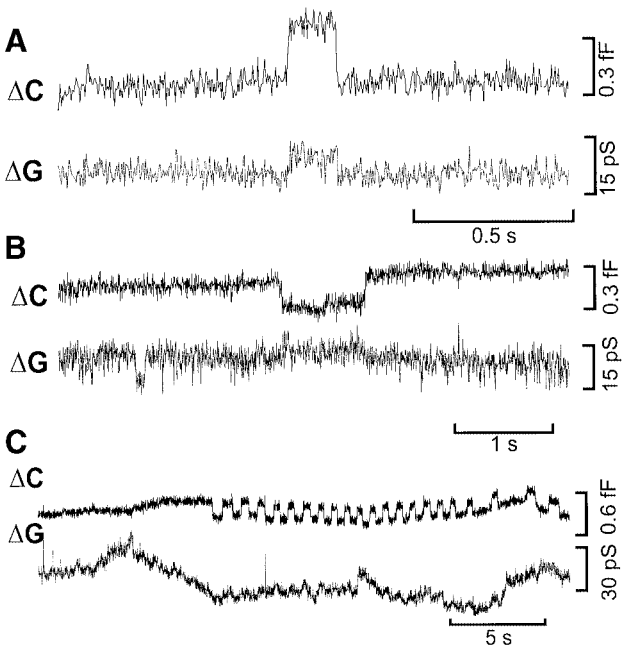

Fig. 2. Capacitance flicker. (**A**) Transient upward step; (**B**) transient downward step; (**C**) repeated cycles of up- and downward steps characteristic of a flicker burst. (A–C) are each from a different cell.

increase in conductance (arrow) caused either by the opening of ion channels in the patch or by a temporary leak in the seal. At the same time, a current flowed from the bath or from the cell into the pipet. In the original trace, there were small simultaneous deflections in the ΔC trace but these had been eliminated here by optimization of the phase setting (see Materials and methods). Recordings as in Figure 1A typically continued for 15–20 min.

Figure 1B divides the ΔC trace into segments to show it at higher magnification and time resolution. Several deflections appear that are not readily seen in Figure 1A; five of them (indicated by numbers) passed our criteria for capacitance steps (see Materials and methods) and may represent single endo- and exocytic events. Figure 1C shows each deflection at still higher gain, along with the accompanying ΔG trace. Regression lines (dashed) were fitted to the ΔC segments indicated by horizontal bars in Figure 1C1; they formed the basis for deciding whether or not to accept the step and for determining its amplitude. Three downward and two upward steps suggest three endo- and two exocytic events, respectively.

Often a ΔC step was followed by another of similar amplitude but opposite direction ('capacitance flicker'), as if either an exocytic vesicle fused with the plasmalemma but then disconnected (Figure 2A) or an endocytic vesicle budded off the plasmalemma and then reconnected (Figure 2B). Note that both the transient upward and downward ΔC steps in Figure 2B were associated with a transient increase in the ΔG trace, indicating that the fusion pore connecting the vesicle in Figure 2A remained narrow and failed to dilate fully, and that the 'fission pore' connecting the endocytic vesicle in Figure 2B constricted but did not close completely (see later). ΔG changes as large as these were not always observed.

More rarely, upward and downward ΔC steps alternated rhythmically. Since it is highly unlikely that different vesicles result in alternating up- and downward steps of

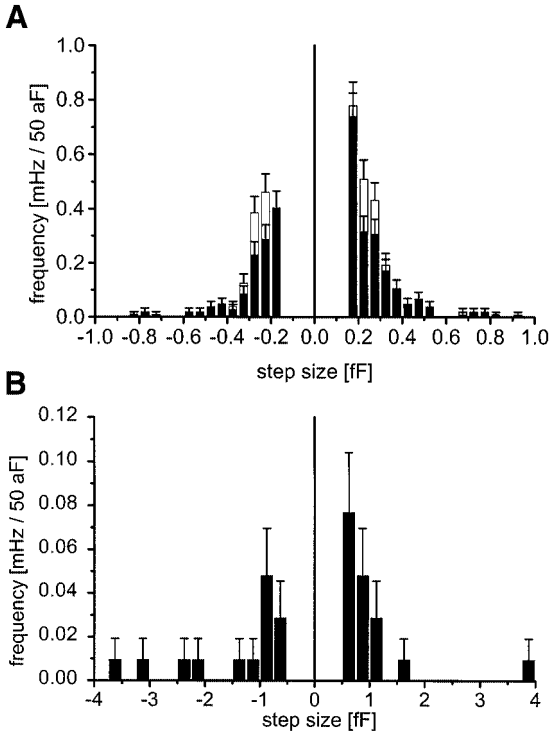

Fig. 3. Step amplitude distribution in chromaffin cells. From recordings as in Figures 1 and 2. (**A**) Steps <0.5 fF, detected as described in Materials and methods. Open bars include all steps passing the selection criteria, including those during flicker bursts as in Figure 2C. Black bars: steps in flicker bursts were excluded except for the first cycle of up–down or down–up pairs. Negative values indicate downward and positive values upward steps. Error bars give the square root of the step count in each bin, scaled to units of frequency. To obtain frequency, counts were divided by total recording time (29.4 h at an r.m.s. noise level of 0.05 fF or better in 106 cells). (**B**) Steps between 0.5 and 4 fF sorted into 0.25 fF bins; ordinates were divided by 5 to make frequencies applicable to 0.05 fF bins as in (A).

such similar amplitudes, we suggest that a single vesicle repeatedly broke and re-made an electrical connection with the cell surface (Figure 2C). A more thorough description of such capacitance flicker is given later. Bursts of flicker were seen in five of 106 cells. Although times between up and down steps varied considerably from episode to episode, individual open and close times were closely similar within the same flicker burst (see later, Figure 4).

Spontaneous exo- and endocytosis involve small vesicles

Recordings were made from 106 patches, each on a different cell and yielding from 177 to 1670 s of recording (total 29.4 h) at an r.m.s. noise level of <0.05 fF. The number of exo- and endocytic events was plotted as a histogram in Figure 3A (white bars) with ΔC steps sorted into 0.05 fF bins. Amplitudes were plotted positive for exo- and negative for endocytic steps. Since steps <0.15 fF could not be detected reliably, they were not counted even though their frequency may well be high. It is clear nonetheless that most steps in Figure 3A must represent structures smaller than large dense-core granules. Dense-core granules have a mean diameter of ~300 nm in electron micrographs (Parsons *et al.*, 1995; Plattner *et al.*, 1997), and each contributes an average of ~2 fF (Neher and Marty, 1982; Albillos *et al.*, 1997; Moser and Neher, 1997). The great majority of exo- and endocytic steps were <0.4 fF, and the highest frequency steps had amplitudes of ≤0.15 fF. With a membrane capacitance of 10 fF/μm^2, spherical vesicles of 0.15–0.4 fF capacitance would have diameters of 70–110 nm. We suggest that most steps in Figure 3A result from the constitutive endo- and exocytosis of small vesicles. Based on their size, most endocytic events in Figure 3A could be clathrin mediated. Larger steps were exceedingly rare (Figure 3B). Only six endo- and four exocytic steps >1.0 fF were seen in this data set.

Even though flicker bursts were rare, they accounted for a significant portion of the steps in Figure 3A (white bars). The black bars result from eliminating steps in flicker bursts. They include the first opening or closing of a vesicle as well as the first subsequent step, if any, even if it was in the opposite direction. However, they exclude all subsequent actions of a flickering vesicle. All black bars together correspond to frequencies of one endocytic step every 14 min (1.2 mHz) and one exocytic step every 9 min (1.8 mHz).

Next, steps passing our selection criteria were re-examined visually and selected only when there was no sign of a step in the opposite direction in 3 s intervals either before or afterwards. On average, there was one such solitary exocytic step every 11 min (1.5 mHz) and one solitary endocytic step every 22 min (0.8 mHz). Comparing these frequencies with those given above suggests that 15% of exo- and 35% of endocytic steps were transient.

The low step frequencies are averages, include recordings with no steps at all (35 of 106 patches) and contrast with Figure 1B where five steps occurred in ~5 min. Most probably exo- and endocytic events occur preferentially at discrete locations on the cell surface, as in clathrin-mediated endocytosis (Gaidarov *et al.*, 1999). Thirty-two out of 106 patches had only exocytic and 10 only endocytic steps. At a local level, therefore, exo- and endocytosis are not necessarily in balance.

Constitutive membrane turnover is slow in resting chromaffin cells

We calculated the surface represented by the steps included in Figure 3A (black bars). In 29.4 h of recording, the total amount of membrane exocytosed during events between 0.15 and 0.5 fF was 38.5 fF, and that endocytosed was 17.4 fF. These values must be divided by 0.5 since most steps <0.5 fF are detected with ~50% efficiency (see later). The result is 77 fF for exo- and 35 fF for endocytosis. Larger vesicles exocytosed 18 fF and endocytosed 25 fF in the same patches; we expect to have detected them all. Hence we estimate that a total of 95 fF were added by exocytosis and 60 fF withdrawn by endocytosis. Exo- and endocytosis were not exactly in balance, possibly because mechanical effects of the cell-attached pipet favored exo- over endocytosis. The average of the two values is 77 fF. The analysis suggests that a patch containing 6 μm^2 of membrane (see Materials and methods) with 60 fF capacitance turns over its membrane ~77/60 = 1.3 times in 29 h, or about once a day at 20–23°C. The figure could be somewhat larger because steps <0.15 fF are missed in

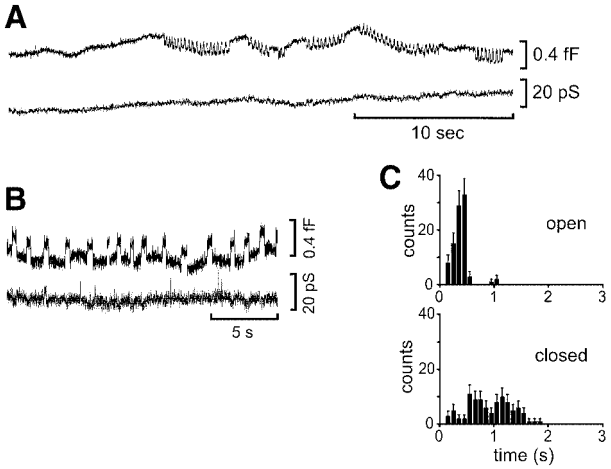

Fig. 4. Staurosporine-induced capacitance flicker. Standard bath solution with 2 μM staurosporine. (**A**) Probable instance of frustrated endocytosis. Upper trace, Δ*C*; lower trace, Δ*G*. The trace starts 398 s after the beginning of the recording; prior to the episode shown, there were no episodes of flicker by other vesicles. (**B**) As in (A) but magnified and from a different cell. Note the regular rhythm of up- and downward steps. (**C**) Histograms of open times (Δ*C* trace high) and closed times (Δ*C* trace low) from an episode including the trace in (B). The timing of Δ*C* steps was determined as described in Materials and methods, except that the presence or absence of a step was decided by inspection.

our recordings. Turnover is also expected to be faster at 37°C (Matlin and Simons, 1983).

We calculated the volume associated with each downward step (black bars in Figure 3A) assuming that endocytic vesicles are spheres surrounded by membrane of 10 fF/μm^2 specific capacitance. After correcting for our detection efficiency, the sum from all recorded steps of <0.5 fF in Figure 3A (black bars) was 0.112 fl. The relatively few larger steps took up as much volume, 0.12 fl, bringing the total to 0.23 fl/patch in 29.4 h. If a patch is representative of the entire plasma membrane and contains 1% of a chromaffin cell's surface, then each cell endocytoses 23 fl in 29.4 h, or 0.9 fl/h.

Our estimate includes transient endocytic events that would not cause uptake of extracellular marker, and it fails to include transient exocytic events that would. Apart from flicker bursts, about one-third of exo- and endocytic events are transient. Our estimate is inaccurate in so far as the additional volume imported in transient fusion cannot be expected to equal exactly that attributed erroneously to transient fission events.

Staurosporine causes endocytic events to become transient

In the presence of staurosporine (2 μM), the occurrence of prolonged episodes of capacitance flicker became more frequent. Figure 4A shows an example. A downward step occurred about midway through the trace and initiated a long sequence of alternating up- and downward steps. As in Figure 2C, we suggest that a single vesicle repeatedly attempted to disconnect its lumen from the external space but succeeded only for short periods. Bursts of such 'capacitance flicker' alternated with periods of silence. In our data set of 14 staurosporine-treated cells, eight cells (or 57%) showed flicker bursts, compared with only 6% in the absence of the drug.

Table I. Effect of staurosporine on flicker bursts and solitary steps

	No drug		Staurosporine	
Flicker bursts:				
burst time (%)	0.58 ± 0.4	106 cells	14.5 ± 7.3	14 cells
burst duration (s)	20.1 ± 5.4	8 bursts	54.4 ± 27.8	21 bursts
open time (s)	0.44 ± 0.13	8 bursts	0.55 ± 0.08	21 bursts
closed time (s)	1.39 ± 0.29	8 bursts	1.5 ± 0.25	21 bursts
step size (fF)	0.21 ± 0.02	8 bursts	0.31 ± 0.05	21 bursts
Solitary steps:				
size (fF)	0.27 ± 0.01	241 steps	0.32 ± 0.05	11 steps
Step frequency (mHz)	2.3 ± 0.1	241 steps	1.1 ± 0.3	11 steps

In a burst, at least three steps of alternating direction must follow their predecessor within 3 s and satisfy the criteria outlined in Materials and methods. Any period longer than 3 s between qualifying steps was taken to terminate a burst. Solitary steps must neither follow, nor be followed by, a visually detected step of opposite direction within 3 s. Burst time is the percentage of time in each cell where at least one vesicle is engaged in a burst. Open refers to the time the capacitance is high, closed to when it is low in recordings as in Figures 2C or 4B. The step sizes given are the average of mean step amplitudes in each burst, or the average of solitary steps in each condition.

For analysis, a flicker burst was defined as containing at least four steps alternating in direction, each step following its predecessor within 3 s. Table I summarizes the properties of bursts both with and without staurosporine. The drug strongly increased the fraction of time where at least one vesicle is engaged in a burst. It had lesser or no effects on the other variables in Table I. The mean step amplitudes are similar or identical to that of solitary steps. With staurosporine, there are fewer solitary steps, as if at least some bursts of transient closings and openings occur at the expense of the complete fusions and fissions seen without drug. The last two findings are consistent with the idea that the same types of vesicles successfully complete exo- and endocytosis in the absence of the drug. However, they fail to do so in the presence of staurosporine and instead they lapse into a flickering mode. Flicker with the drug appears similar to the flicker occasionally recorded without the drug, except for a difference described later. We cannot rule out that staurosporine also induces a completely new exo–endocytic mechanism.

Vesicles close and re-open rhythmically

Figure 4B shows a segment of a burst at higher magnification. Again, alternating up- and downward Δ*C* steps of very similar amplitude suggest that the fission pore of a single vesicle repeatedly opened and closed, or dilated and constricted. Figure 4C shows histograms for the 'open time' of this burst (where the Δ*C* level was high and the vesicle presumably connected to the extracellular space) and for the closed time. The open time histogram in particular showed a pronounced peak. Both histograms differ strongly from those obtained for the stochastic opening and closing of ion channels (summarized, for example, in Colquhoun and Hawkes, 1981). Evidently fission pores in endocytic vesicles may open and close rhythmically rather than stochastically.

Staurosporine hinders complete vesicle closure

Do flicker bursts result from exocytic vesicles failing to open fully, from endocytic vesicles failing to close fully,

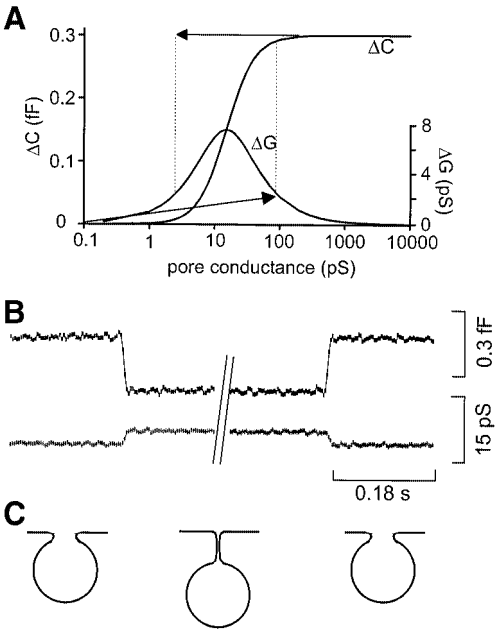

Fig. 5. Incomplete fusions and fissions cause ΔG steps. (**A**) Real (ΔG) and imaginary parts of the electrical admittance (ΔC) are calculated for a typical 0.3 fF vesicle and an excitation frequency of 8 kHz, and plotted against the conductance of the aqueous pore connecting the vesicle lumen with the external space. The equations are $\Delta C = 2\pi f C_v/z$ and $\Delta G = [(2\pi f C_v)^2/g\ ]/z$ where C_v is the capacitance of the vesicle, f the frequency of the sinusoid, g the pore conductance and $z = [(2\pi f C_v/g)^2 + 1]$ (see, for example, Breckenridge and Almers, 1987). A vesicle fusing with the plasma membrane (rightward arrow) would start with both ΔG and ΔC equal to zero. As its fusion pore opens to, for example, 100 pS, ΔC increases by nearly 0.3 fF while a ΔG deflection of ~2 pS remains. Both ΔC and ΔG vary in parallel. A vesicle budding off the plasma membrane and forming a fission pore of 2pS (leftward arrow) would start with $\Delta G = 0$ and cause a drop in ΔC by ~0.3 fF, but as long as its pore conductance remains finite, a ΔG deflection also remains. ΔG and ΔC vary in opposite directions. (**B**) Average time course of down- and upward steps in the episode shown in Figure 4B, calculated as follows. We divided the ΔC and ΔG traces into 300 ms segments, one ΔC–ΔG pair for each upward step and one pair for each downward step. Segments containing downward steps were aligned to the falling phases of ΔC and averaged, those with upward steps were treated similarly. The result (left) shows ΔC and ΔG deflections at greatly diminished noise levels. (**C**) Possible morphological basis of the electrical events in (B).

or both? Flicker bursts caused by an endocytic vesicle start with a downward step, and those caused by an exocytic vesicle start with an upward step. However, this distinction cannot be made in most recordings in staurosporine as these start in the middle of a burst. The calculation plotted in Figure 5A illustrates an alternative method to distinguish a vesicle trying to undergo fusion from one trying to undergo fission.

A vesicle fusing with the plasma membrane but opening incompletely is expected to cause an upward ΔC step accompanied by an upward ΔG step (right-pointing arrow). The ΔG step represents the appearance of an electrical conductance connecting the vesicle lumen to the outside, namely the conductance of the fusion pore while it has not dilated fully (e.g. Breckenridge and Almers, 1987; Zimmerberg *et al.*, 1987). ΔG vanishes when the pore conductance becomes too large to support a significant voltage difference under sinusoidal excitation. By contrast, when a vesicle buds from the cell surface or when it constricts an initially wide connection with the external space, the result is a downward ΔC step accompanied by a ΔG increase (left-pointing arrow in Figure 5A). Now the ΔG step represents the resistance of the aqueous connection, called the fission pore (Rosenboom and Lindau, 1994). ΔG vanishes when the fission pore has closed completely. Hence ΔC and ΔG will vary in parallel when a vesicle fuses without opening completely, and in opposite directions when a vesicle tries to undergo fission without closing completely.

ΔG and ΔC changes during flicker bursts were compared. In most recordings, deflections in the ΔG trace seemed lost in noise. To make them more visible, all segments containing steps were excised from a burst, aligned to the times of capacitance steps, and both the ΔC and ΔG segments thus aligned were averaged. The result of such an analysis for the vesicle in Figure 4C is shown in Figure 5B. ΔG increased while ΔC fell.

The ΔG deflection is not the result of an incorrect phase setting. To make the ΔG deflection disappear, the phase would have to be ~17° more negative. However, when the ΔC and ΔG traces were re-calculated with this new phase, the ΔC trace showed deflections that were correlated temporally with the opening and closing of ion channels elsewhere in this trace (not shown). Since ion channels change only the conductance and not the capacitance, the more negative phase setting must be incorrect. With the new phase, the ΔC changes were also correlated temporally with the ΔG changes. To find out by how much the new phase was in error, we plotted ΔC against ΔG while ion channels opened and closed (not shown). The regression line formed an angle of $-20 \pm 2°$ with the abscissa ($p < 0.0001$); hence the new phase was –20° too negative and the phase originally used in Figure 5B was within 3° of being correct. Evidently, ΔG and ΔC deflections of this vesicle were genuinely in opposite directions, consistent with a vesicle closing transiently and incompletely.

The traces in Figure 5B are consistent with a vesicle of 0.27 fF capacitance constricting a fission pore down to a conductance of only 4 pS. Figure 5C shows a possible morphological basis for the vesicle in Figure 5B. In other vesicles, no ΔG deflection could be detected even after signal averaging multiple steps. These vesicles must either have closed completely or their fission pore conductance was <1 pS.

In 15 of 22 flicker bursts with staurosporine, ΔG and ΔC varied in the opposite direction, in six ΔG did not vary measurably and in only one did ΔG and ΔC vary in parallel. In the absence of the drug, ΔG and ΔC changes were parallel in three of eight vesicles, opposite in four of eight vesicles and in one ΔG did not vary measurably. Apparently, the predominant effect of staurosporine is to prevent vesicles from closing their fission pore completely. Hence the drug may be viewed as an inhibitor of endocytosis.

Our step selection erroneously rejects half of the small capacitance steps

To avoid contaminating our ΔC step count by noise, we applied stringent step selection criteria (see Materials and methods) that most probably made us reject some genuine steps. Flicker episodes provide an opportunity to test how many steps are falsely rejected since, during flicker, rhythmically repeating steps of similar or identical ampli-

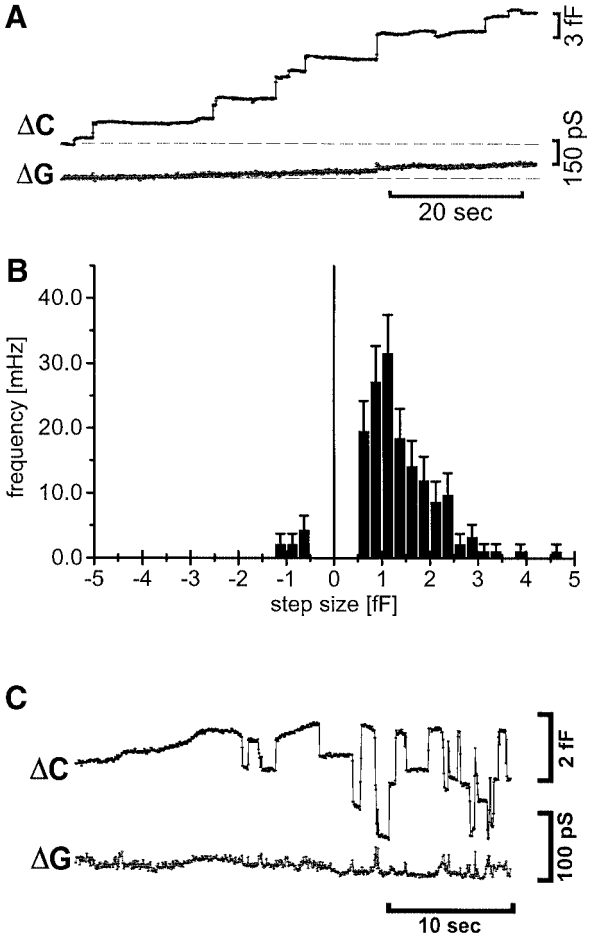

Fig. 6. Capacitance steps in stimulation buffer. (**A**) A cell showing an unusually large number of large exocytic steps. (**B**) A histogram from two such cells, with the ordinate scaled as in Figure 3B. Note the preponderance of exocytic steps. Large (>0.5 fF) upward steps occurred 17 times more frequently than in the other 43 cells from this data set. (**C**) Capacitance flicker in the presence of 2 μM staurosporine. Upper, Δ*C*; lower, Δ*G*.

tudes are easily recognized visually even if they do not pass all criteria of automated selection. We inspected traces as in Figures 2C or 4A and B and with step amplitudes from 0.15 to 0.3 fF. Steps were detected visually and their number was compared with the number of steps detected by our selection algorithm. The algorithm accepted 64 ± 13% of transitions in staurosporine (mean step amplitude 0.19 ± 0.01 fF in nine bursts) and 45 ± 7% without the drug (eight bursts; mean step amplitude 0.21 ± 0.02 fF).

Staurosporine also induces flicker in large vesicles

Unlike the recordings discussed so far, those of Albillos *et al.* (1997) showed frequent large upward steps that represented exocytosis of dense-core granules as they were accompanied by quantal release of catecholamine. This was confirmed when we made recordings under conditions similar to those of Albillos *et al.* (1997) in an external solution that encouraged exocytosis of dense-core granules as it contained elevated [Ca^{2+}] and the K channel blocker tetraethylammonium. In a total of 2 h of recordings from 43 cells, exocytic steps with amplitudes between 0.5 and 4 fF appeared at 10 times higher frequency than even

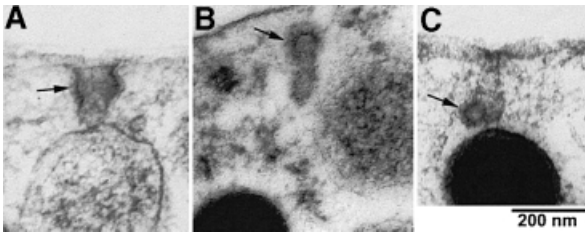

Fig. 7. Endocytic organelles in chromaffin cells. Rapidly frozen, 100 nm thick sections. Arrows indicate the possible clathrin coat. Note open endocytic vesicles in (**A**) and (**C**), and the large dense-core granules in (**B**) and (C).

the smallest steps in standard bath solution. Recordings from two cells showed particularly high exocytic step frequency; one is shown in Figure 6A. The step size histogram for exocytosis in the two cells showed a peak at ~1.2 fF (Figure 6B), as in the histogram of Albillos *et al.* (1997) and at values nearly 10 times higher than the exocytic steps in Figure 3.

Figure 6C was recorded under identical conditions but in the presence of staurosporine. After 6 min of silence, a downward step in the Δ*C* trace initiated flicker of an ~1 fF vesicle. Since downward steps of this size were exceedingly rare in normal bathing solution, those in Figure 6C are most probably a consequence of stimulating exocytosis of LDCVs. It probably marks the closing of an LDCV that had performed exocytosis earlier and whose cavity had remained intact and connected to the cell surface. Soon other vesicles of at least three different sizes joined. Δ*C* steps are accompanied by transient deflections in the Δ*G* trace, as expected if aqueous connections to the vesicle cavities dilated and constricted gradually (Albillos *et al.*, 1997). In most cases, multiple vesicles started to flicker soon after the first vesicle started, and continued until the end of the recording. Flicker was not obviously rhythmic. Apart from this difference, however, the recording suggests that staurosporine affects large and small vesicles similarly. Of 16 cells in the presence of staurosporine, 13 showed flicker, and in 11 of them multiple large vesicles flickered simultaneously. Without the drug, short flickers of single vesicles were observed in only two of 45 cells.

Endocytic organelles in chromaffin cells

Although endocytic events are rare in resting chromaffin cells, endocytic structures near the plasma membrane were observed occasionally. Figure 7 shows three examples in quickly frozen sections, two of them still open to the external space (Figure 7A and C). Coats possibly representing clathrin are seen to cover portions of the structures. Comparable structures were also seen in stimulated chromaffin cells (Patzak and Winkler, 1986). The structures are not spherical. If they are approximated as cylinders, their surface areas would be in the range 0.020–0.033 μm^2, and would result in 0.20–0.33 fF downward steps when they disconnect from the cell surface.

Discussion

Cells continuously renew their plasma membrane through constitutive exo- and endocytosis. In chromaffin cells,

constitutive plasma membrane turnover has not been studied in detail, as attention has focused on calcium-triggered exocytosis and the membrane retrieval that follows it (Henkel and Almers, 1995). Nonetheless, resting chromaffin cells readily take up extracellular marker and hence perform constitutive endocytosis (von Grafenstein and Knight, 1993). In cell-attached patch–clamp recordings, we found that the plasma membrane capacitance spontaneously diminished in small steps, as if due to the retrieval of <0.04 μm^2 membrane pieces caused by endocytosis of <110 nm diameter spherical vesicles. The events detected by us (0.015–0.040 μm^2) would result in a volume uptake of ~0.9 fl/h per cell, similar to the 1.2 fl/h per cell observed previously with extracellular markers (von Grafenstein and Knight, 1993; their Figure 2a). We also observed endocytic structures by electron microscopy in resting chromaffin cells. The structures were partially coated and their surface area was of the order of 0.02–0.03 μm^2. Hence the downward capacitance steps observed here most probably represent single events of constitutive endocytosis because they have the size expected from endocytic organelles in chromaffin cells, and are predicted to result in a volume uptake as found with extracellular markers.

The organelle for constitutive exocytosis has not been characterized in chromaffin cells. In embryonic chick myotubes, 100 nm diameter vesicles are thought to carry nicotinic acetylcholine receptors to the plasma membrane (Bursztajn and Fischbach, 1984) while virus-infected BHK-21 cells contain 50–100 nm diameter vesicles thought to carry viral protein to the plasma membrane (Griffiths *et al.*, 1985). Hence vesicles for constitutive exocytosis in these cells are 50–100 nm in diameter, and increase the cell surface in 0.008–0.031 μm^2 steps on exocytosis. By analogy, we expect the plasma membrane capacitance of chromaffin cells to increase in 0.08–0.31 fF steps. Our method does not reliably detect 0.08 fF steps and would miss most of the smallest vesicles in BHK-21 cells. Nonetheless, spontaneous upward steps were observed, and the vast majority had amplitudes of 0.15–0.4 fF, similar to those predicted from morphological studies. It seems likely that the spontaneous upwards steps in capacitance represent single constitutive exocytic events.

Rhythmic closing and opening of endocytic vesicles

Remarkably often, exo- and especially endocytic events appeared transient. Sometimes vesicles rhythmically opened and closed, or dilated and constricted their connection to the external space. This surprising behavior became dominant in the presence of the protein kinase inhibitor staurosporine. It was never seen when patch pipets were sealed onto silicone beads (see Materials and methods), hence it cannot be an instrumentation artifact. The rhythmic closing and opening of fission pores is in striking contrast to the stochastic opening and closing of single ion channels. Open time histograms of single channels have their highest value at infinitesimally short intervals and then fall exponentially at longer times. In contrast, both open and closed time histograms for rhythmically opening vesicles showed a peak. In the presence of staurosporine, the transient closing events during a flicker burst often were accompanied by an increase in the ΔG trace, suggesting that an endocytic vesicle was closing incompletely.

Rhythmic closing and opening is strongly stimulated by staurosporine, but is also seen occasionally in the absence of the drug. The finding is reminiscent of 'potocytosis' (Anderson *et al.*, 1992), a hypothesis postulating the rhythmic opening and closing of caveolae to explain folate uptake. However, protein kinase C inhibits potocytosis by inhibiting the internalization of caveolae (Smart *et al.*, 1994), and hence the kinase inhibitor staurosporine is expected to stimulate internalization and hence the fission of the vesicle. This would be opposite to what the present results suggest. It remains unknown whether the rhythmic opening and closing is related to potocytosis, whether it has a physiological purpose or whether it represents a rare malfunction resulting from an underdamped biochemical feedback cascade.

On a molecular level, the rhythmic behavior will require a long sequence of reactions with similar rate constants before a final event constricts the access pore of a vesicle. It will require a similarly long sequence before a final and most likely different reaction opens the vesicle. It is difficult at present to speculate on this point. Endocytosis is thought to happen in two steps. First the endocytic vesicle (Figure 5C, left) is pulled away from the cell surface and the membranous neck that still connects it lengthens and narrows (Figure 5C, middle; see also Stowell *et al.*, 1999). Next the neck is broken and the vesicle disconnects. If staurosporine prevents the neck from being broken and if the force pulling the vesicle exists for a fixed time only, the vesicle might re-approach the plasma membrane and its neck might shorten and widen again (Figure 5C, right). For instance, a large number of dynamin molecules are thought to assemble, probably sequentially, to form a spiraling collar around the neck of a vesicle (Hinshaw and Schmid, 1995; Takei *et al.*, 1995). The collar was suggested to force the vesicle away from the plasma membrane when it autocatalytically hydrolyzes GTP and lengthens suddenly (Stowell *et al.*, 1999). However, another protein probably is required to disconnect the vesicle completely (Sever *et al.*, 1999). If it is inhibited by staurosporine, the vesicle may fail to disconnect before the dynamin collar disassembles again. An alternative hypothesis may envisage the vesicle pulled away from the plasma membrane in small sequential steps, either by a myosin crawling processively along an actin filament or by the polymerization of G-actin monomers. The vesicle may re-approach the plasma membrane when the force on the vesicle subsides, either because polymerization stops or because the tension on the vesicle becomes so high that the myosin lets go. None of the three hypotheses explains all features of rhythmic flicker bursts, and the molecular mechanism may not be known for some time. Nonetheless, the finding suggests that endocytosis is based on a reaction sequence that may function as a chemical oscillator. The actin polymerization-driven movement of *Listeria* becomes pulsatile with N-terminal deletions in the bacterial protein ActA (Lasa *et al.*, 1997).

Effects of staurosporine on exo- and endocytosis

At the frog nerve–muscle synapses, staurosporine was reported to prevent the escape of FM1-43 from synaptic vesicles, while allowing the escape of neurotransmitter

(Henkel and Betz, 1995). FM1-43 is a lipidic dye and it was suggested that vesicles release transmitter without mixing their lipid and flattening into the cell surface ('kiss-and-run' exocytosis, Fesce *et al.*, 1996). Recent work on hippocampal neurons has confirmed that synaptic vesicles can remain connected to the cell surface for seconds, retain some of their FM1-43 and then disconnect again in a rapid phase of 'endocytosis' that is hastened by staurosporine (Klingauf *et al.*, 1998). At synapses, staurosporine can be viewed as inhibiting the final step in exocytosis, namely full fusion of the exocytic vesicle with the plasma membrane. A second effect of staurosporine is more likely to be related to the cytoskeleton or to proteins that bind vesicles to the cytoskeleton. When synaptic vesicles are newly formed by endocytosis, they fail to mix into the pool of pre-existing vesicles when the drug is present (Kraszewski *et al.*, 1996).

In the present work, the dominant effect of the drug was to inhibit a late step in endocytosis, namely the separation of endocytic vesicle from the plasma membrane. Inhibition of endocytosis is suggested by a difference between flicker bursts with and without staurosporine. With the drug, ΔC and ΔG tend to change in opposite directions, as expected from vesicles trying unsuccessfully to close, while without the drug parallel and antiparallel changes in ΔC and ΔG were about equally frequent. Endocytic action in staurosporine became repetitive, transient and often demonstrably incomplete.

In summary, staurosporine inhibits closure of vesicles in chromaffin cells, hastens endocytosis in hippocampal neurons and inhibits the full opening of synaptic vesicles during exocytosis in motor neurons. At the concentrations used in this and the previous work, staurosporine is expected to inhibit many protein kinases, and this may wholly or in part account for the variety of effects. The findings suggest that phosphorylation influences multiple steps in endo- and exocytosis to different degrees in different cells.

Materials and methods

Bovine chromaffin cells (BCCs) were prepared and cultured as described (Parsons *et al.*, 1995), and used 2–5 days after preparation. The standard bath solution contained, in mM: 150 NaCl, 2 KCl, 2 $MgCl_2$, 2 $CaCl_2$, 10 HEPES–NaOH buffer pH 7.2. Staurosporine (Calbiochem) was kept as a 2 mM stock solution in dimethylsulfoxide (DMSO). Recording pipets (borosilicate glass, wall thickness 0.3 mm, o.d. 2 mm) were pulled with a micropipet puller (Flaming/Brown, Model P-97), coated with wax (Kerr®, Sybron). They were fire-polished immediately before use and filled with bath solution; their resistances were then 1.5–3 MΩ. Pipets were sealed against the membranes of chromaffin cells to isolate electrically beneath them a membrane patch for 'cell-attached recording'. Patches were held at a d.c. potential of +20 mV relative to the bath, making the potential across the membrane patch (cytosol minus pipet) 20 mV more negative than elsewhere on the plasma membrane. Photomicrographs (100× oil objective, NA 1.3) showed the pipets to have opening diameters of 1.5–2 μm, corresponding to an opening of 2–3 μm^2 cross-sectional area. The patch was larger than the cross-sectional area of the pipet tip because the plasmalemma bulged into the opening. If hemispherical, the bulge would have a surface of 3.5–6 μm^2, ~0.5–1% of the area of a typical chromaffin cell. All experiments were carried out at 20–23°C. Electron microscopy was carried out as described (Parsons *et al.*, 1995; Tse *et al.*, 1997).

Capacitance measurements

Changes in the electrical capacitance of the membrane patch were used as an assay for changes in patch surface area due to exo- and endocytic events. Capacitance changes (ΔC) were measured with a lock-in amplifier (SR830-DSP; Stanford Research Systems, Stanford, CA) set to a time constant of 0.3 ms and connected to an EPC-7 patch–clamp run at full bandwidth and a gain of 50 mV/pA or higher. An 8 kHz sine wave of 240 mV peak-to-peak amplitude was superimposed onto the d.c. potential applied to the pipet. In-phase (ΔG, conductance) and 90°C out-of-phase (ΔC, capacitance) signals were filtered with a four-pole Bessel filter at 160 Hz, and sampled and written to disk at 333 Hz each by a Labmaster A/D converter (Axon Instruments, Burlingame, CA) in a computer running DOS 6.0. The patch current and voltage were filtered at 200 Hz and also recorded at 333 Hz each; after the filter, line frequency interference was removed from the current signal with a signal processor (HumBug, Quest Scientific). Recording and analysis were performed with software written by A.W.Henkel.

At the beginning of a recording, the C_{fast} setting on the EPC-7 patch–clamp amplifier was changed repeatedly by 3 fF with a push button installed for this purpose. The phase setting was adjusted until this maneuver produced no deflections on the ΔG trace. The phase shift ϕ_0 thus required was $\phi_0 = -45°$ and compensated for electronic delays in the EPC-7 and for the delayed charging of the pipet capacitance (~4.5 pF) through the feedback resistor of the amplifier. During data analysis, it appeared that this setting was imperfect, as it did not completely prevent conductance changes from feeding into the ΔC signal. To find a more appropriate phase shift, we chose segments of the recording where spontaneous single channel activity or temporary seal instabilities caused fluctuations in the ΔG trace. Caused entirely by conductance changes, such events should not cause fluctuations in the ΔC trace, and the best phase setting should be one that minimizes noise in such a ΔC segment. To find this, we re-computed the ΔG and ΔC traces (Lindau, 1991) with an additional phase shift, ϕ:

$$\Delta G_{corr.} = \Delta G \times \cos(\phi) + \Delta C \times \sin(\phi)$$

$$\Delta C_{corr.} = -\Delta G \times \sin(\phi) + \Delta C \times \cos(\phi)$$

The calculation was repeated as ϕ was varied in 1° steps from –90 to 90°C. For each ΔC trace thus calculated, we measured the r.m.s. noise. The phase shift resulting in the lowest r.m.s. ΔC noise was taken as optimal, and was typically 2–20° more negative than ϕ_0.

Capacitance step detection

After phase correction, the ΔC trace was scanned for up- and downward steps possibly representing exo- and endocytic events (see also Hartmann *et al.*, 1995). A computer program first loaded a pair of ΔC and ΔG data segments (10 000 points each) from disk into memory. For each point, n, it averaged four adjacent ΔC points, (ΔC_{n-3} to ΔC_n), as well as the next four (ΔC_{n+1} to ΔC_{n+4}). If the difference of the means had an absolute value >0.1 fF, it was tentatively assumed that a step had occurred between points n and $n + 1$. Regression lines were fitted through 150 ms segments both before and after the putative step (see Figure 1C), i.e. through points ($n - 50$) to n and through points ($n + 2$) to ($n + 52$). The program then measured the slopes of the regression lines, their vertical distance (step amplitude) at point $n + 1$, and the r.m.s. noise of the ΔC points about the ΔC regression lines. Similar regression lines were also fit to the ΔG traces. The step was accepted if it satisfied the following criteria. (i) The ΔC r.m.s. noise about both regression lines was <0.05 fF; (ii) the amplitude of the ΔC step was between 0.15 and 1 fF; (iii) the ΔC step amplitude was at least three times larger than that of the accompanying ΔG step, if any; (iv) the slopes of the ΔC regression lines differed by <3.2 fF/s; and (v) the step did not result from lock-in amplifier resets or manual capacitance compensations carried out from time to time. If all criteria were met, the accompanying ΔC and ΔG segments were saved in a separate file, and the program resumed step detection after skipping four points (points $n + 1$ to $n + 5$ in our example). Our criteria were strict and recognized only about half of all ΔC steps actually occurring (see Results).

We used slightly different criteria to detect capacitance steps larger than 0.5 fF, because during exo- and endocytosis ΔC changes tend to spread out in time as fusion and fission pores slowly change conductances. Traces were plotted on a chart recorder and screened by eye for large C steps. If a step was detected, the segment containing the step was loaded into computer memory. Regression lines were fitted as above, except that a longer interval of 10 ms was allowed between the end of the pre-step regression line and the step, and an interval of 40 ms between the step and the post-step regression line. This allowed conductance changes in fusion pores to run their course. Then the noise about the regression lines and the step amplitude was measured as above. Steps were accepted if their amplitudes were between 0.5 and 4 fF, if their amplitude exceeded

the noise about the regression lines at least 4-fold and if the ΔC regression lines before and after a step differed in slope by <3.2 fF/s.

To calculate the average frequency of steps, we measured the time during which the recording noise was low enough for steps to satisfy our selection criteria. We divided ΔC traces into 100 ms segments, fitted each by a straight line and measured the r.m.s. fluctuations about that line. Segments with noise of maximally 0.05 fF were accepted. On average, this was true ~90% of the time.

To test how often steps may be the chance result of recording noise, small balls of polymerized silicone resin (Sylgard) were prepared as follows. The tip of a fine syringe needle was bent into a small metal loop, and the loop dipped into a mixture of 1 ml of silicone rubber compound RTV615A and 100 µl of curing agent RTV615B (General Electric). The silicone formed a bead around the metal loop that was hardened for 5 min in a hot air stream. The bead was submerged in standard bath solution and a seal was formed with a patch pipet as if the silicone ball were a cell. To set the phase optimally, we proceeded as with cells, using recording segments where the pipet was withdrawn slightly to reduce the seal resistance to <5 GΩ. In 14 h of recording, three upward steps (0.28 ± 0.04 fF) and eight downward steps (0.36 ± 0.09 fF) passed all our selection criteria. Their combined frequency (0.22 ± 0.07 mHz) may be taken to represent a lower limit on what may be detected in living cells. It was not increased by staurosporine and was significantly lower than in chromaffin cells.

Recording steps under conditions favoring exocytosis of dense-core granules

Experiments were carried out in a solution similar to that used by Albillos *et al.* (1997). Our bath solution contained (in mM) 120 NaCl, 10 $CaCl_2$, 2 KCl, 2 $MgCl_2$, 20 tetraethylammonium (TEA), 5.5 glucose, 10 HEPES–NaOH pH 7.4. The pipet solution was identical except that it lacked glucose and contained additionally 0.1 mM carbachol. The lock-in amplifier used an 8 kHz sine wave of 50 mV peak-to-peak, and had its output time constant set to 3 ms. The voltage, ΔC and ΔG signals were not filtered; current was filtered at 100 Hz. Each of the four signals was sampled at 25 Hz. ΔC and ΔG traces were analyzed automatically as above except that regression lines were fitted to 375 ms segments each before and after the step [points (n – 14) to n and (n + 4) to (n + 19)]. Steps were accepted if their amplitudes were between 0.5 and 4.0 fF, if they exceeded the noise by at least 4-fold and if the regression lines differed in slope by <6.4 fF/s.

Acknowledgements

This work was supported by HFSP grant # RG0197.

References

Albillos,A., Dernick,G., Horstmann,H., Almers,W., Alvarez de Toledo,G. and Lindau,M. (1997) The exocytotic event in chromaffin cells revealed by patch amperometry. *Nature*, **389**, 509–512.

Ales,E., Tabares,L., Poyato,J.M., Valeor,V., Lindau,M. and Alvarez de Toledo,G. (1999) High calcium concentrations shift the mode of exocytosis to the kiss-and-run mechanism. *Nature Cell Biol*., **1**, 40–44.

Alvarez de Toledo,G., Fernandez-Chacon,R. and Fernandez,J.M. (1993) Release of secretory products during transient vesicle fusion. *Nature*, **363**, 554–558.

Anderson,R.G., Kamen,B.A., Rothberg,K.G. and Lacey,S.W. (1992) Potocytosis: sequestration and transport of small molecules by caveolae. *Science*, 255, 410–411.

Breckenridge,L.J. and Almers,W. (1987) Currents through the fusion pore that forms during exocytosis of a secretory vesicle. *Nature*, **328**, 814–817.

Bursztajn,S. and Fischbach,G.D. (1984) Evidence that coated vesicles transport acetylcholine receptors to the surface membrane of chick myotubes. *J. Cell Biol*., **98**, 498–506.

Colquhoun,D. and Hawkes,A.G. (1981) On the stochastic properties of single ion channels. *Proc. R. Soc. Lond. B Biol. Sci*., **211**, 205–235.

Fernandez,J.M., Neher,E. and Gomperts,B.D. (1984) Capacitance measurements reveal stepwise fusion events in degranulating mast cells. *Nature*, **312**, 453–455.

Fesce,R., Valtorta,F. and Meldolesi,J. (1996) The membrane fusion machine and neurotransmitter release. *Neurochem. Int*., **28**, 15–21.

Gaidarov,I., Santini,F., Warren,R.A. and Keen,J.H. (1999) Spatial control of coated-pit dynamics in living cells. *Nature Cell Biol*., **1**, 1–7.

Griffiths,G., Pfeiffer,S., Simons,K. and Matlin,K. (1985) Exit of newly synthesized membrane proteins from the *trans* cisterna of the Golgi complex to the plasma membrane. *J. Cell Biol*., **101**, 949–964.

Hartmann,J., Szepek,S. and Lindau,M. (1995) Regulation of granule size in human and horse eosinophils by number of fusion events among unit granules. *J. Physiol*., **483**, 201–209.

Henkel,A.W. and Betz,W.J. (1995) Staurosporine blocks evoked release of FM1-43 but not acetylcholine from frog motor nerve terminals. *J. Neurosci*., **15**, 8246–8258.

Henkel,A.W. and Almers,W. (1996) Fast steps in exocytosis and endocytosis studied by capacitance measurements in endocrine cells. *Curr. Opin. Neurobiol.*, **6**, 350–357.

Hinshaw,J.E. and Schmid,S.L. (1995) Dynamin self-assembles into rings suggesting a mechanism for coated vesicle budding. *Nature*, **374**, 190–192.

Hörber,H.J.K., Mosbacher,J. and Häberle,W. (1995) Force microscopy on membrane patches. In Sakmann,B. and Neher,E. (eds), *Single Channel Recordings.* 2nd edn. Plenum Press, New York, pp. 375–393.

Kelly,R.B. (1985) Pathways of protein secretion in eukaryotes. *Science*, **230**, 25–32.

Klingauf,J., Kavalali,E.T. and Tsien,R.W. (1998) Kinetics and regulation of fast endocytosis at hippocampal synapses. *Nature*, **394**, 581–585.

Kraszewski,K., Diell,L., Mundigl,O. and De Camilli,P. (1996) Mobility of synaptic vesicles in nerve endings monitored by recovery from photobleaching of synaptic vesicle-associated fluorescence. *J. Neurosci*., **16**, 5905–5913.

Kreft,M. and Zorec,R. (1997) Cell-attached measurements of attofarad capacitance steps in rat melanotrophs. *Pflugers Arch.*, **434**, 212–214.

Lasa,I., Gouin,E., Goethals,M., Vancompernolle,K., David,V., Vandekerckhove,J. and Cossart,P. (1997) Identification of two regions in the N-terminal domain of ActA involved in the actin comet tail formation by *Listeria monocytogenes*. *EMBO J*., **16**, 1531–1540.

Lindau,M. (1991) Time-resolved capacitance measurements: monitoring exocytosis in single cells. *Q. Rev. Biophys*., **24**, 75–101.

Lollike,K., Borregaard,N. and Lindau,M. (1995) The exocytotic fusion pore of small granules has a conductance similar to an ion channel. *J. Cell Biol*., **129**, 99–104.

Matlin,K.S. and Simons,K. (1983) Reduced temperature prevents transfer of a membrane glycoprotein to the cell surface but does not prevent terminal glycosylation. *Cell*, **34**, 233–243.

Moser,T. and Neher,E. (1997) Estimation of mean exocytic vesicle capacitance in mouse adrenal chromaffin cells. *Proc. Natl Acad. Sci. USA*, **94**, 6735–6740.

Neher,E. and Marty,A. (1982) Discrete changes of cell membrane capacitance observed under conditions of enhanced secretion in bovine adrenal chromaffin cells. *Proc. Natl Acad. Sci. USA*, **79**, 6712–6716.

Parsons,T.D., Coorssen,J.R., Horstmann,H. and Almers,W. (1995) Docked granules, the exocytic burst and the need for ATP hydrolysis in endocrine cells. *Neuron*, **15**, 1085–1096.

Patzak,A. and Winkler,H. (1986) Exocytotic exposure and recycling of membrane antigens of chromaffin granules: ultrastructural evaluation after immunolabeling. *J. Cell Biol.*, **102**, 510–515.

Plattner,H., Artalejo,A.R. and Neher,E. (1997) Ultrastructural organization of bovine chromaffin cell cortex—analysis by cryofixation and morphometry of aspects pertinent to exocytosis. *J. Cell Biol*., **29**, 1709–1717.

Rosenboom,H. and Lindau,M. (1994) Exo–endocytosis and closing of the fission pore during endocytosis in single pituitary nerve terminals internally perfused with high calcium concentrations. *Proc. Natl Acad. Sci. USA*, **91**, 5267–5271.

Scepek,S. and Lindau,M. (1993) Focal exocytosis by eosinophils—compound exocytosis and cumulative fusion. *EMBO J*., **12**, 1811–1817.

Seaman,M.N., Burd,C.G. and Emr,S.D. (1996) Receptor signalling and the regulation of endocytic membrane transport. *Curr. Opin. Cell Biol*., **8**, 549–556.

Sever,S., Muhlberg,A.B. and Schmid,S.L. (1999) Impairment of dynamin's GAP domain stimulates receptor-mediated endocytosis. *Nature*, **398**, 481–486.

Smart,E.J., Foster,D.C., Ying,Y.S., Kamen,B.A. and Anderson,R.G. (1994) Protein kinase C activators inhibit receptor-mediated potocytosis by preventing internalization of caveolae. *J. Cell Biol.*, **124**, 307–313.

Stowell,M.H.B., Marks,B., Wigge,P. and McMahon,H.T. (1999) Nucleotide-dependent conformational changes in dynamin: evidence for a mechanochemical molecular spring. *Nature Cell Biol.*, **1**, 27–32.

Takei,K., McPherson,P.S., Schmid,S.L. and deCamilli,P. (1995) Tubular membrane invaginations coated by dynamin rings are induced by GTPγS in nerve terminals. *Nature*, **374**, 186–190.

Thomas,P., Lee,A.K., Wong,J.G. and Almers,W. (1994) A triggered mechanism retrieves membrane in seconds after Ca^{2+}-stimulated exocytosis in single pituitary cells. *J. Cell Biol.*, **124**, 667–675.

Tse,F.W., Tse,A., Hille,B., Horstmann,H. and Almers,W. (1997) Local Ca^{2+} release from internal stores controls exocytosis in pituitary gonadotrophs. *Neuron*, **18**, 121–132.

von Grafenstein,H. and Knight,D.E. (1993) Triggered exocytosis and endocytosis have different requirements for calcium and nucleotides in permeabilized bovine chromaffin cells. *J. Membr. Biol.*, **134**, 1–13.

Zimmerberg,J., Curran,M., Cohen,F.S. and Brodwick,M. (1987) Simultaneous electrical and optical measurements show that membrane fusion precedes secretory granule swelling during exocytosis of beige mouse mast cells. *Proc. Natl Acad. Sci. USA*, **84**, 1585–1589.

Zupancic,G., Kocmur,L., Veranic,P., Grilc,S., Kordas,M. and Zorec,R. (1994) The separation of exocytosis from endocytosis in rat melanotroph membrane capacitance records. *J. Physiol.*, **480**, 539–552.

Received October 19, 1999; revised November 5, 1999; accepted November 10, 1999